Paper presentation

JACS
JOURNAL OF THE AMERICAN CHEMICAL SOCIETY
pubs.acs.org/JACS

Article

Noncovalent Interactions Steer the Formation of Polycyclic Aromatic Hydrocarbons

Daniël B. Rap, Johanna G. M. Schrauwen, Britta Redlich, and Sandra Brünken*

Cite This: J. Am. Chem. Soc. 2024, 146, 23022–23033
Read Online

Radboud University, FELIX Laboratory, Institute for Molecules and Materials, Toernooiveld 7, 6525 ED Nijmegen, The Netherlands, *E-mail: sandra.bruenken@ru.nl

Soham
08 March 2025

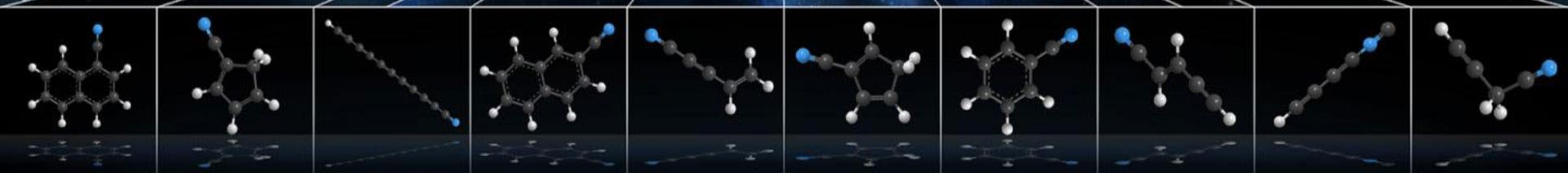

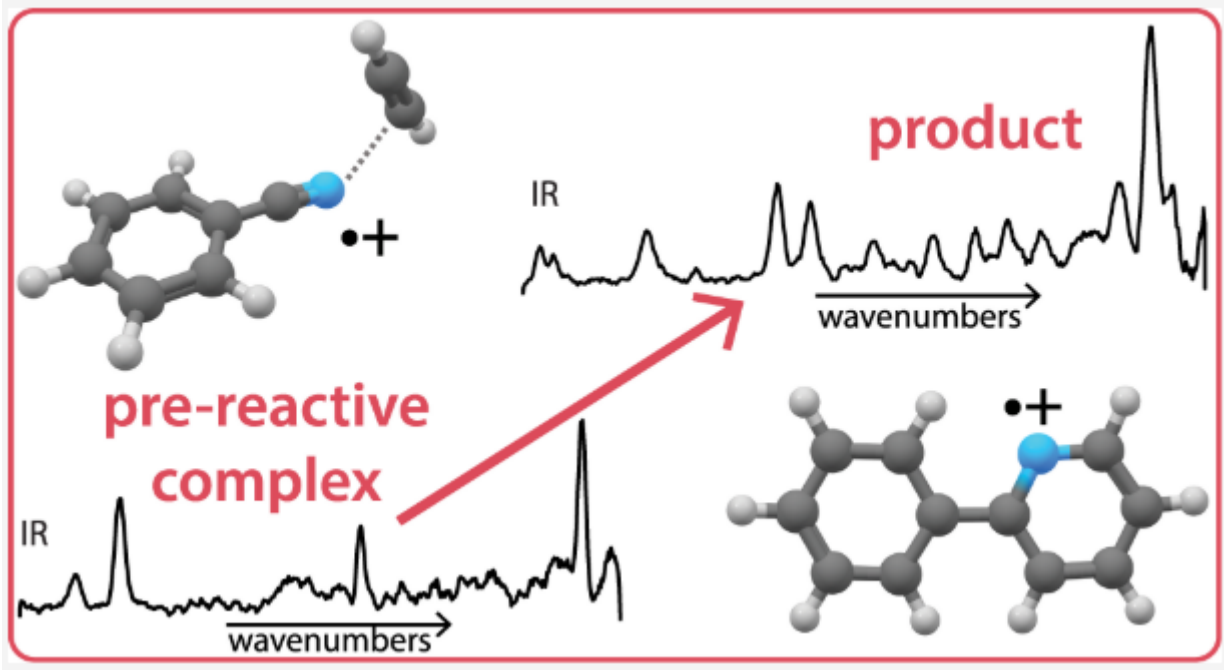
product
IR
wavenumbers
•+
pre-reactive
complex
IR
wavenumbers
•+

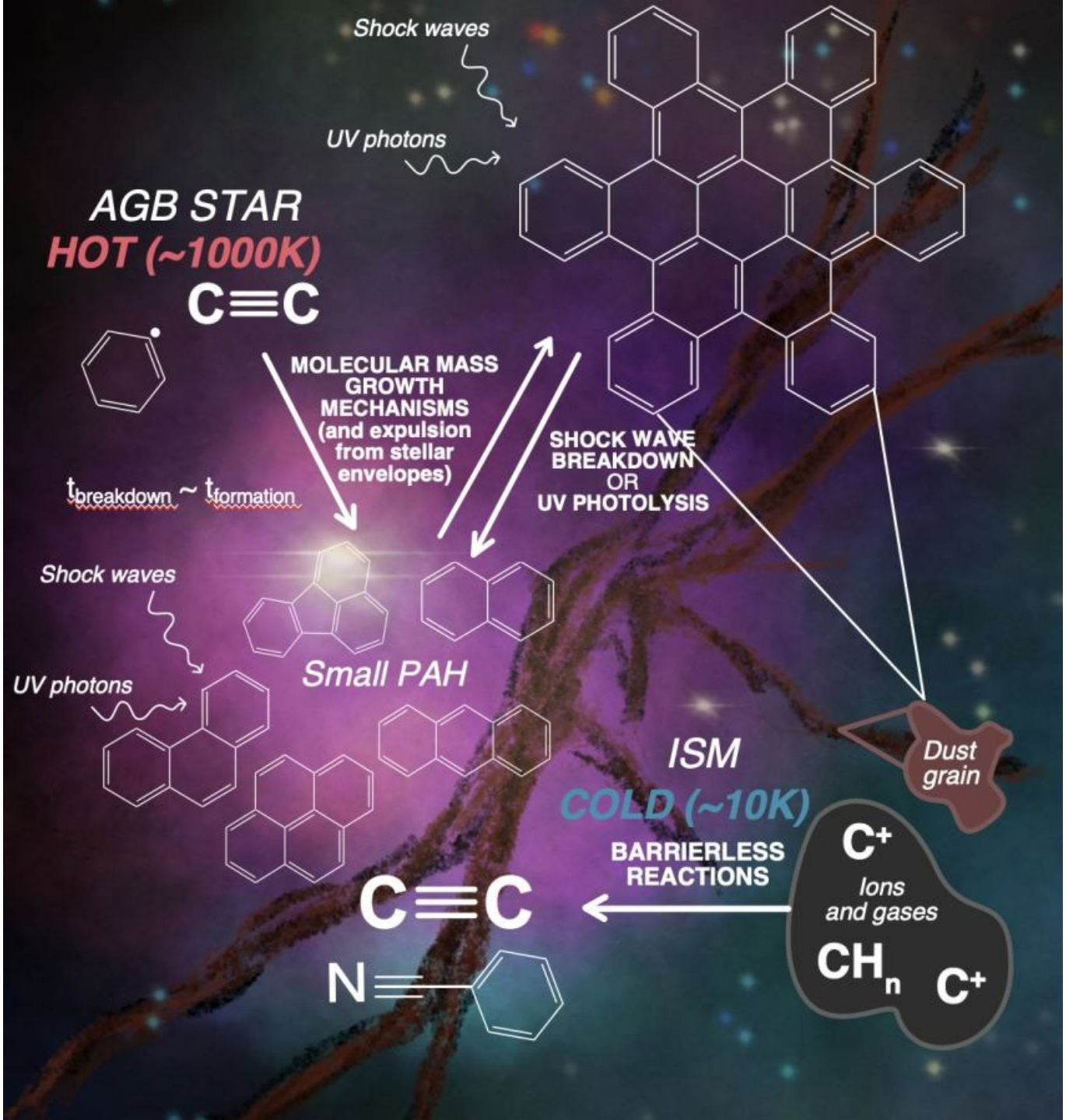
Shock waves
UV photons
AGB STAR
HOT (~1000K)
C≡C
MOLECULAR MASS GROWTH MECHANISMS (and expulsion from stellar envelopes)
SHOCK WAVE BREAKDOWN OR UV PHOTOLYSIS
$t_{breakdown} \sim t_{formation}$
Shock waves
UV photons
Small PAH
ISM
COLD (~10K)
Dust grain
BARRIERLESS REACTIONS
C+
Ions and gases
CH_n C+
C≡C
N≡

Instrumentation

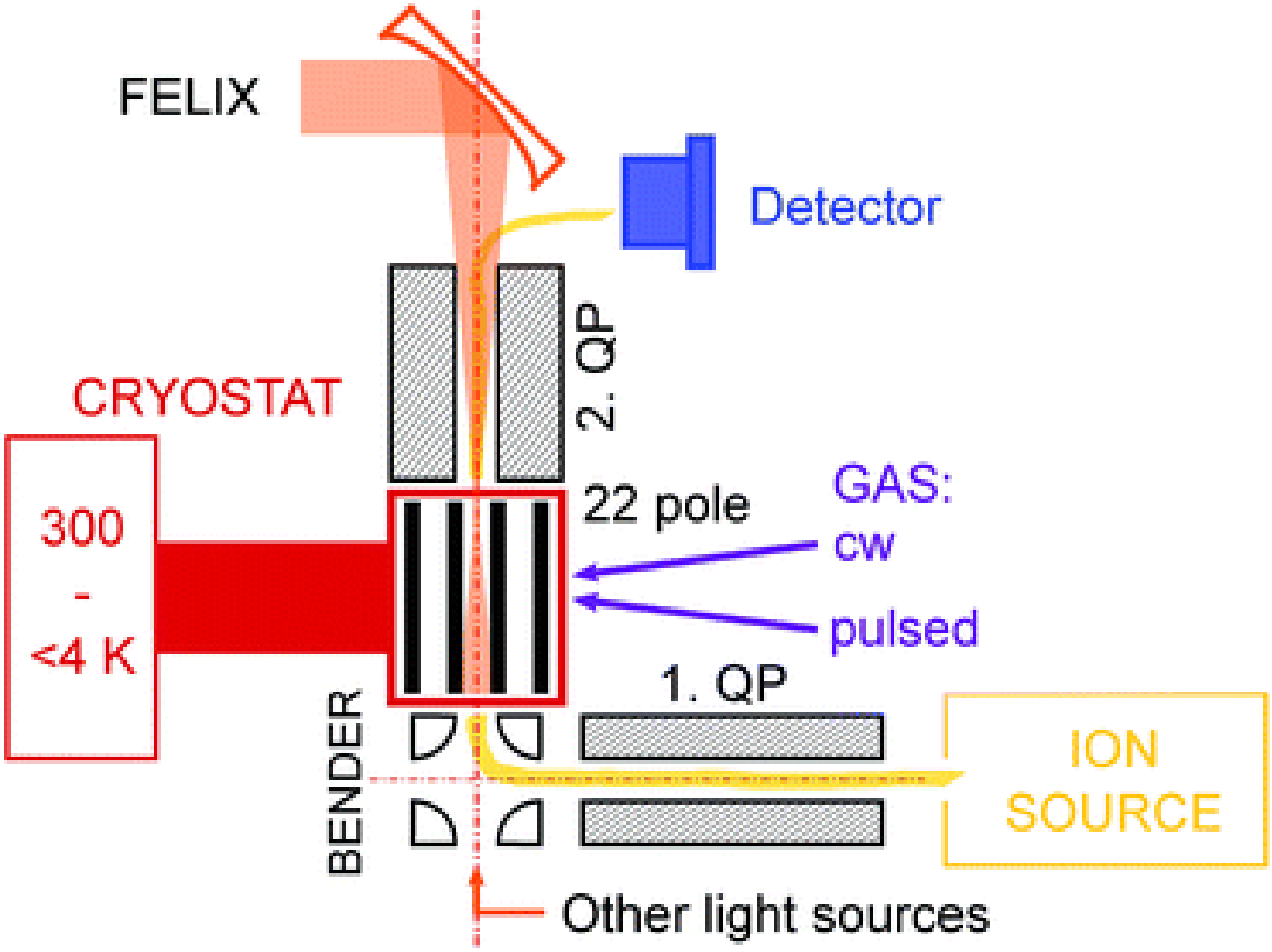

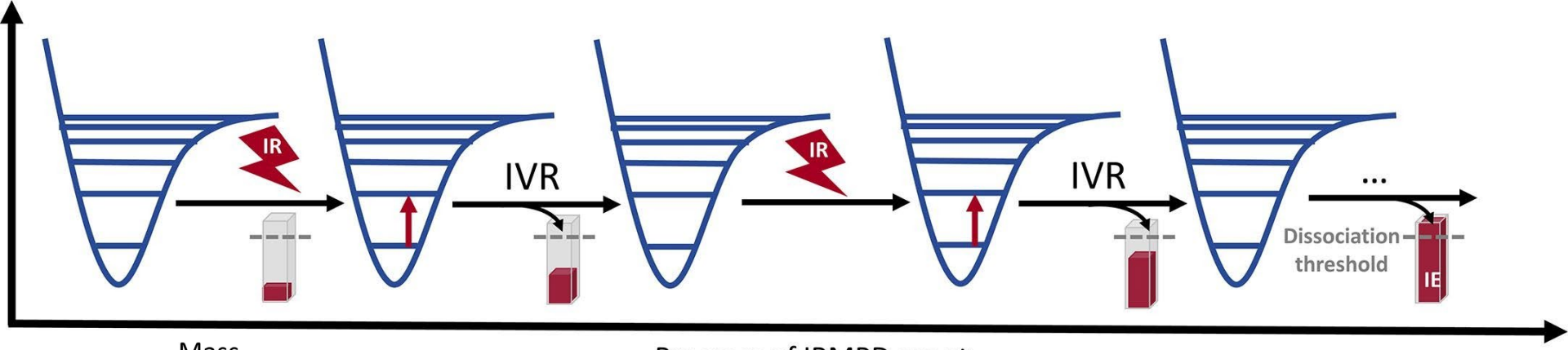

Progress of IRMPD event

irradiation of a molecule, containing a specific vibrational mode, with resonant infrared photons, absorption of a photon causing vibrational excitation, redistribution of the energy via IVR to the internal energy of the molecule causing relaxation of the original electron, and continuation of the cycle until a dissociation threshold is surpassed and dissociation occurs.

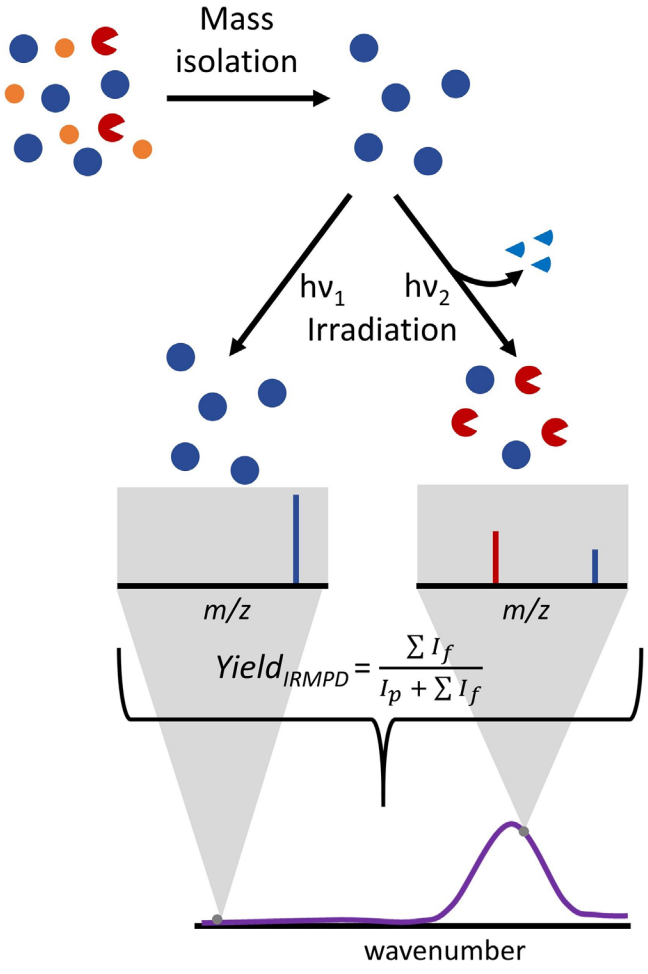

A)

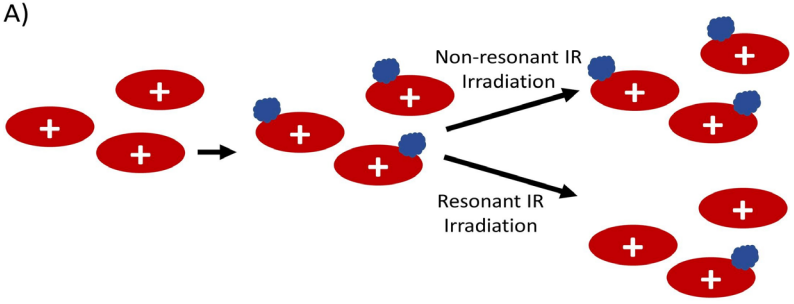

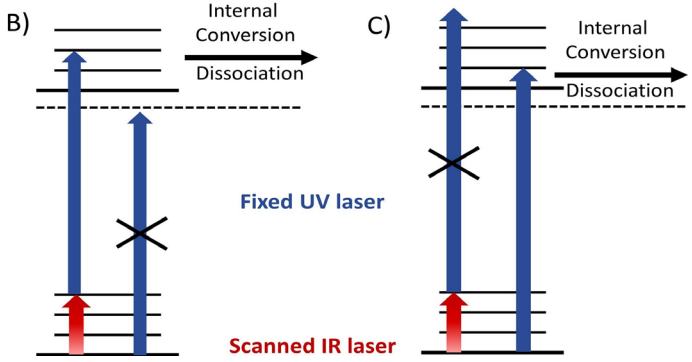

Background

Journal of the American Society for Mass Spectrometry > Vol 17/Issue 4 > Article

Subscribed

Cite Share Jump to Expand

RESEARCH ARTICLE | April 1, 2006

An ICR study of ion-molecules reactions relevant to titan's atmosphere: An investigation of binary hydrocarbon mixtures up to 1 Micron

Vincent G. Anicich, Paul F. Wilson, and Murray J. McEwan

Journal of the American Chemical Society > Vol 135/Issue 1 > Article

Subscribed

Cite Share Jump to Expand

ARTICLE | December 3, 2012

Formation of Nitrogen-Containing Polycyclic Cations by Gas-Phase and Intracluster Reactions of Acetylene with the Pyridinium and Pyrimidinium Ions

Abdel-Rahman Soliman[†], Ahmed M. Hamid[†], Isaac Attah[†], Paul Momoh[†], and M. Samy El-Shall[*†‡]

Journal of the American Chemical Society > Vol 139/Issue 34 > Article

Subscribed

Cite Share Jump to Expand

ARTICLE | July 31, 2017

Nucleophilic Aromatic Addition in Ionizing Environments: Observation and Analysis of New C–N Valence Bonds in Complexes between Naphthalene Radical Cation and Pyridine

Roberto Peverati[†‡], Sean P. Platt[§], Isaac K. Attah[§], Saaudallah G. Aziz[∥], M. Samy El-Shall[*§], and Martin Head-Gordon[*†‡]

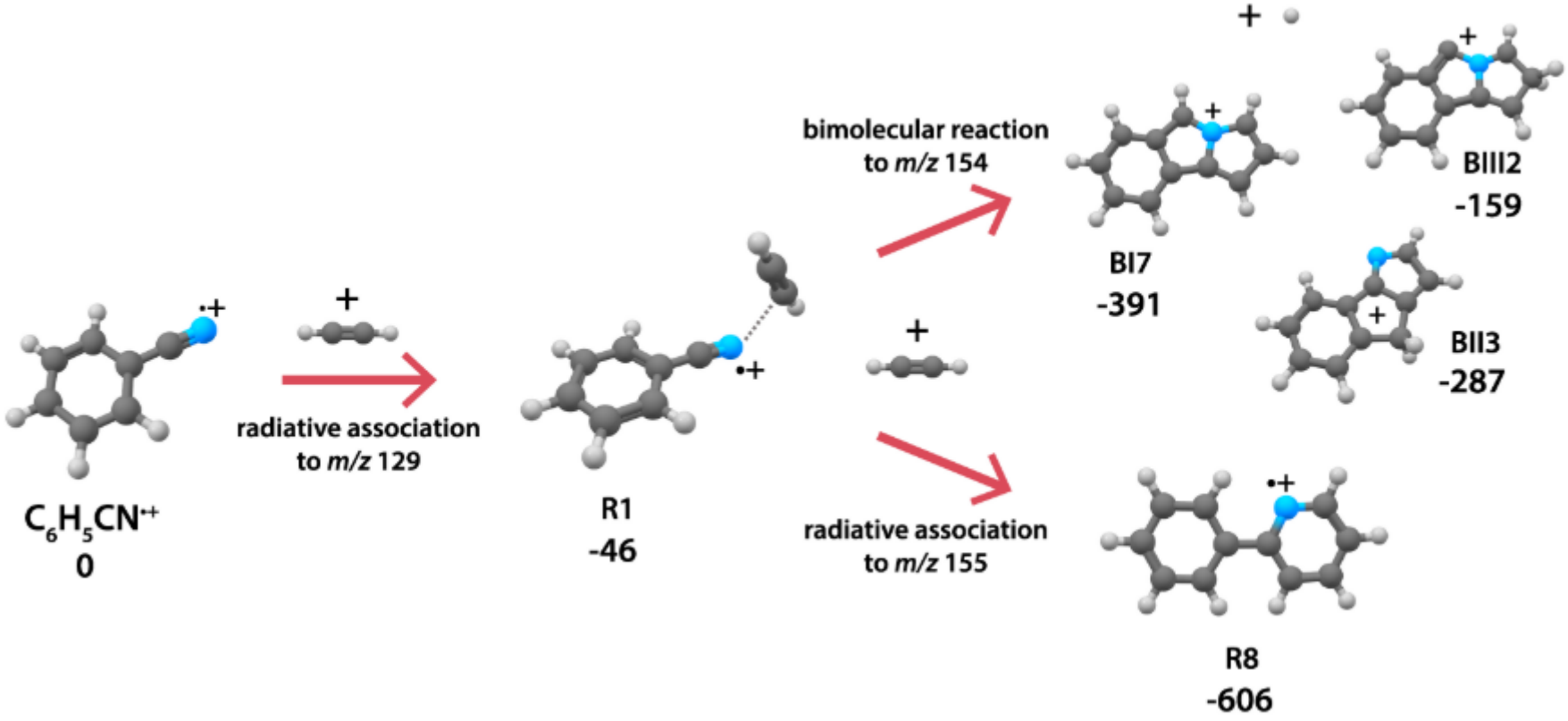

Figure 1. Schematic overview of the overall reaction of benzonitrile$^{\bullet+}$ ($C_6H_5CN^{\bullet+}$) with acetylene (C_2H_2) as spectroscopically determined in this work. Structures of the assigned intermediate **R1** (noncovalent acetylene-benzonitrile$^{\bullet+}$ complex), bimolecular products **BI7**, **BII3**, and **BIII2** (benzo-N-pentalene^{+} isomers) and radiative association product **R8** (2-phenylpyridine$^{\bullet+}$) are shown with energies (in kJ/mol) that correspond to the PES calculations from Figures 4 and 5.

Results

Infrared spectrum of benzonitrile$^{\bullet+}$

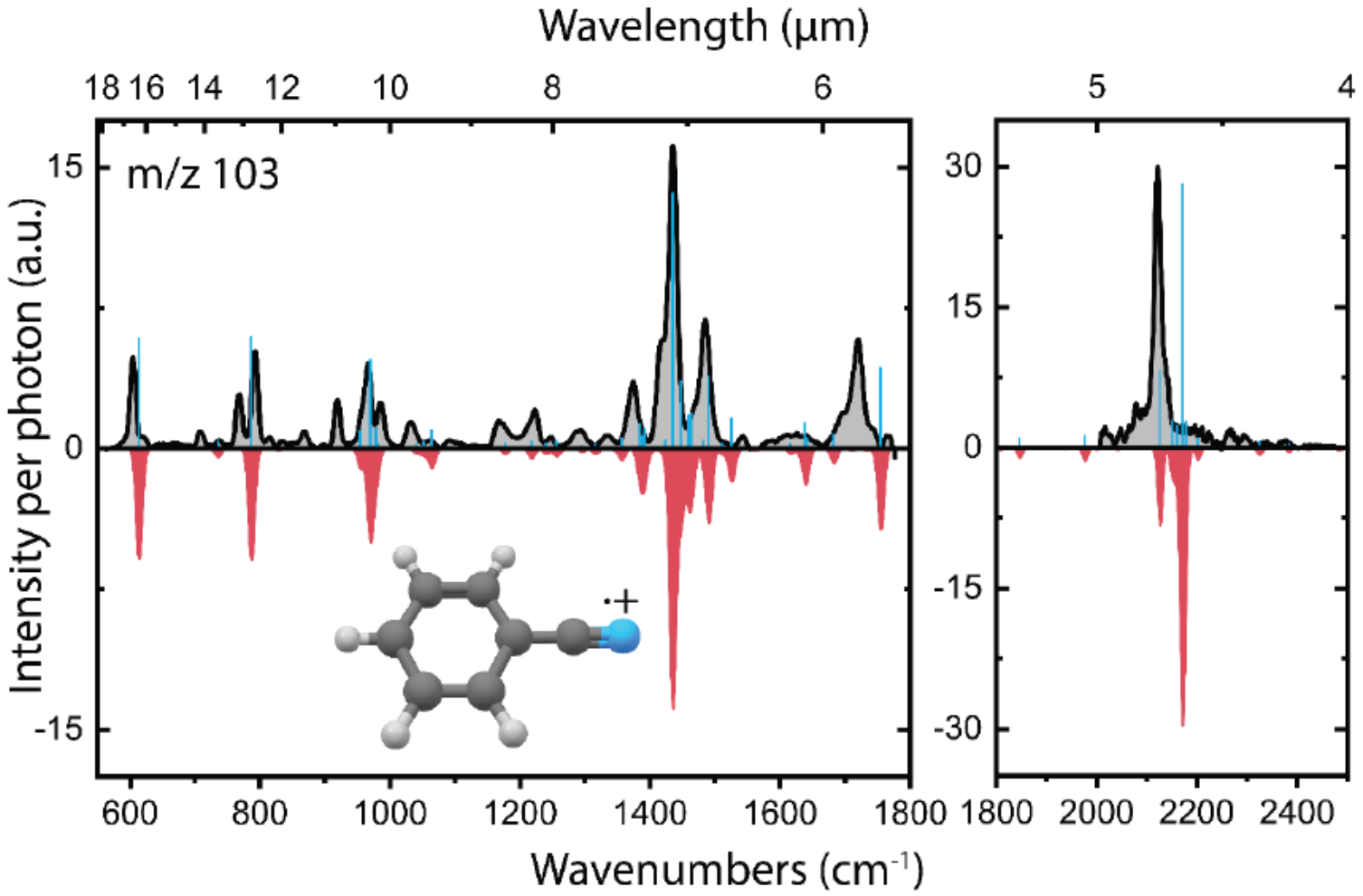

Supplementary Figure 1: Experimental infrared spectrum (grey) of the reactant benzonitrile$^{\bullet+}$ ($C_6H_5CN^{\bullet+}$) with *m/z* 103. The calculated anharmonic infrared frequencies are shown as blue sticks and are convoluted with a Gaussian line-shape with a 5 cm^{-1} width to account for (experimental) broadening effects. The latter is shown as the red spectrum.

The Journal of Physical Chemistry A > Vol 105/Issue 37 > Article

Subscribed

ARTICLE | August 28, 2001

Ionized Benzonitrile and Its Distonic Isomers in the Gas Phase

Robert Flammang, Monique Barbieux-Flammang, Emmanuel Gualano, Pascal Gerbaux, Hung Thanh Le, Minh Tho Nguyen, Frantisek Turecek, and Shetty Vivekananda

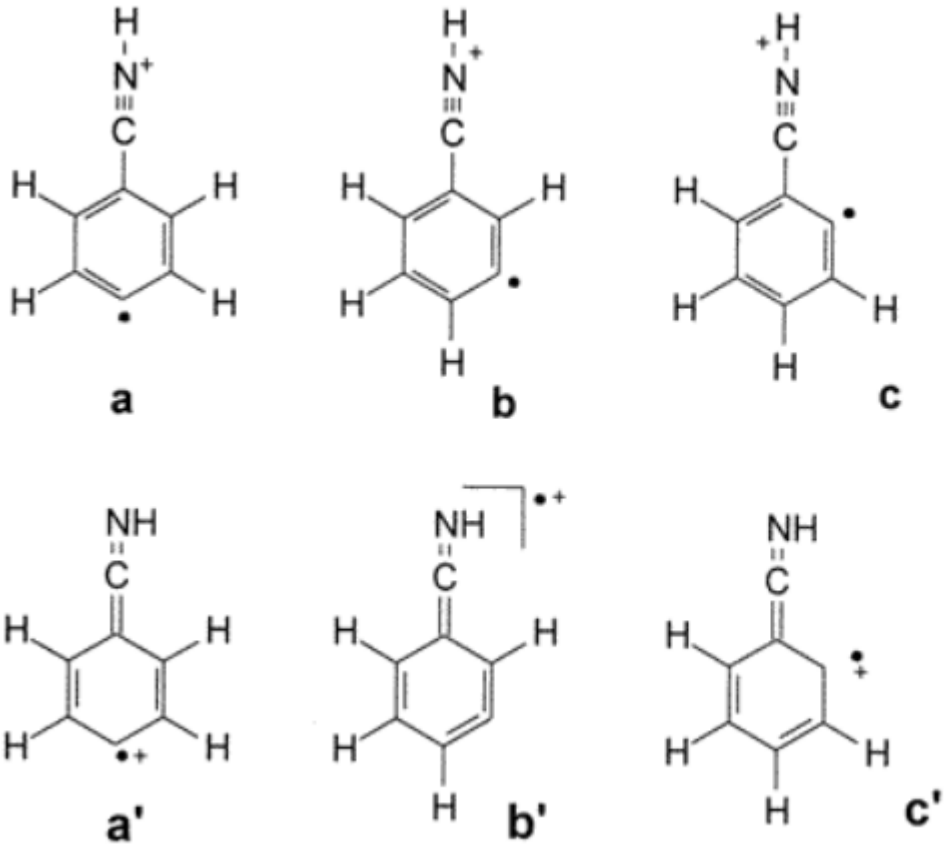

Saturation depletion of benzonitrile$^{\bullet+}$

Details on the saturation depletion method are described in detail by Marimuthu et al.[1] but a brief explanation is given here. Multiple laser pulses, resonant with a vibrational mode of one isomer, are used to burn away the specific isomer from the trap (blue curves, **Supplementary Figure 2 and 3**). As a background measurement, the depletion due to laser heating effects at a non-resonant wavelength is similar determined (orange curves, **Supplementary Figure 2 and 3**). From both measurements, the relative depletion of this isomer can be determined.

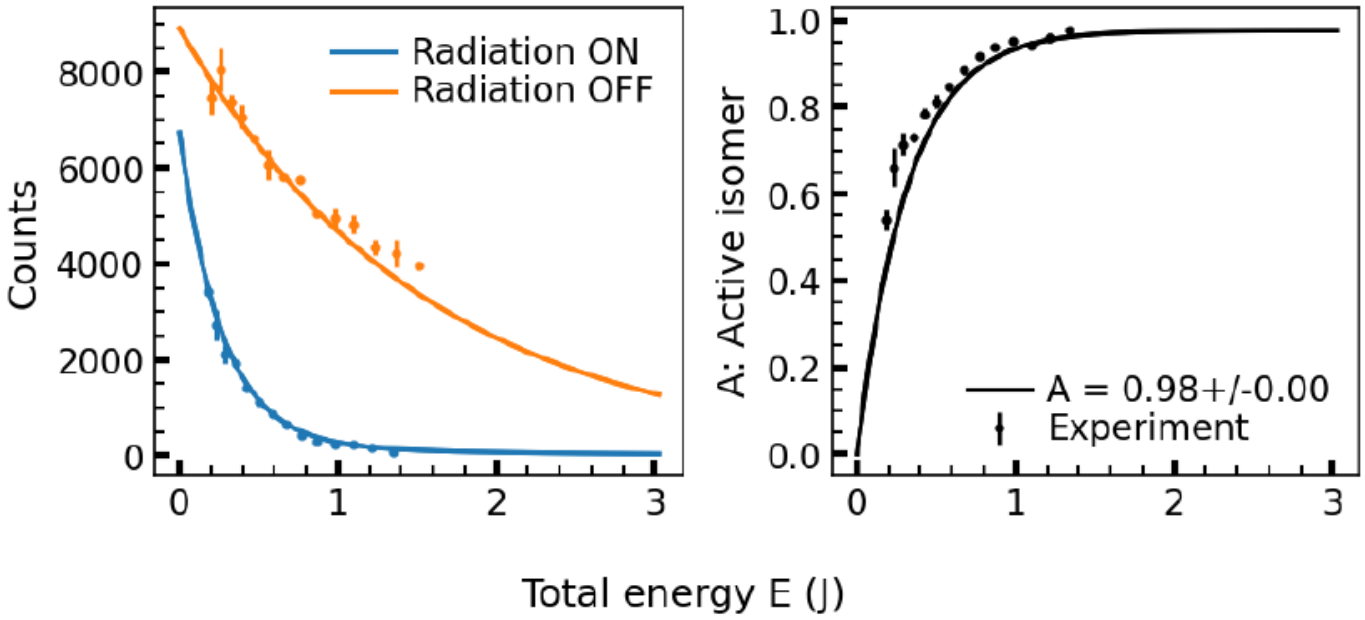

Supplementary Figure 2: Experimental saturation depletion scan of the 920 cm^{-1} mode of benzonitrile$^{\bullet+}$ (*m/z* 103). The on-resonance scan at 920 cm^{-1} (blue) and off-resonance scan at 1010 cm^{-1} (orange) are shown in the left panel. The relative depletion of the active isomer (A) is shown in the right panel as a function of the deposited energy (E). The relative depletion of this band belonging to benzonitrile$^{\bullet+}$ is determined to be 98(±5)%.

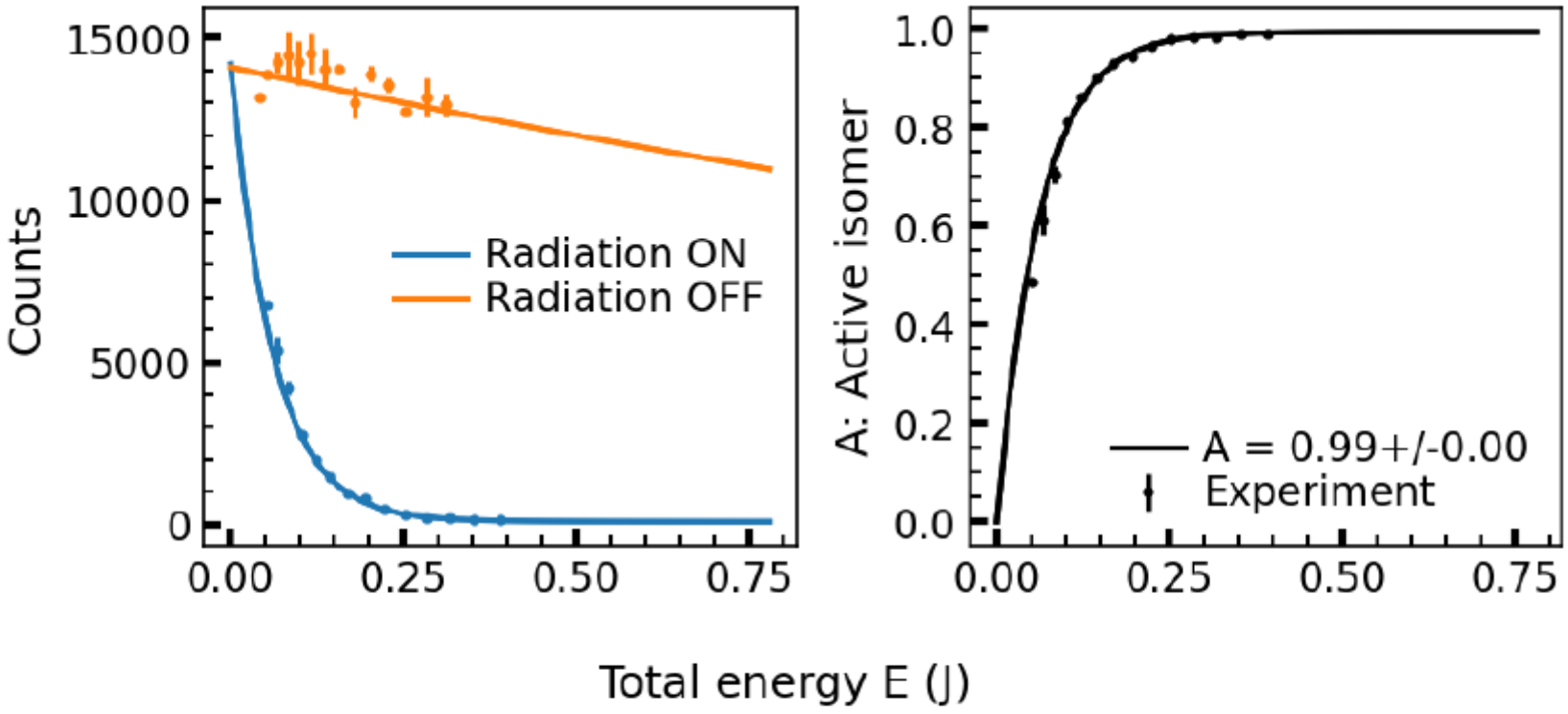

Supplementary Figure 3: Experimental saturation depletion scan of the 1436 cm^{-1} mode of benzonitrile$^{\bullet+}$ (*m/z* 103). The on-resonance scan at 1436 cm^{-1} (blue) and off-resonance scan at 1562 cm^{-1} (orange) are shown in the left panel. The relative depletion of the active isomer (A) is shown in the right panel as a function of the deposited energy (E). The relative depletion of this band belonging to benzonitrile$^{\bullet+}$ is determined to be 99(±5)%.

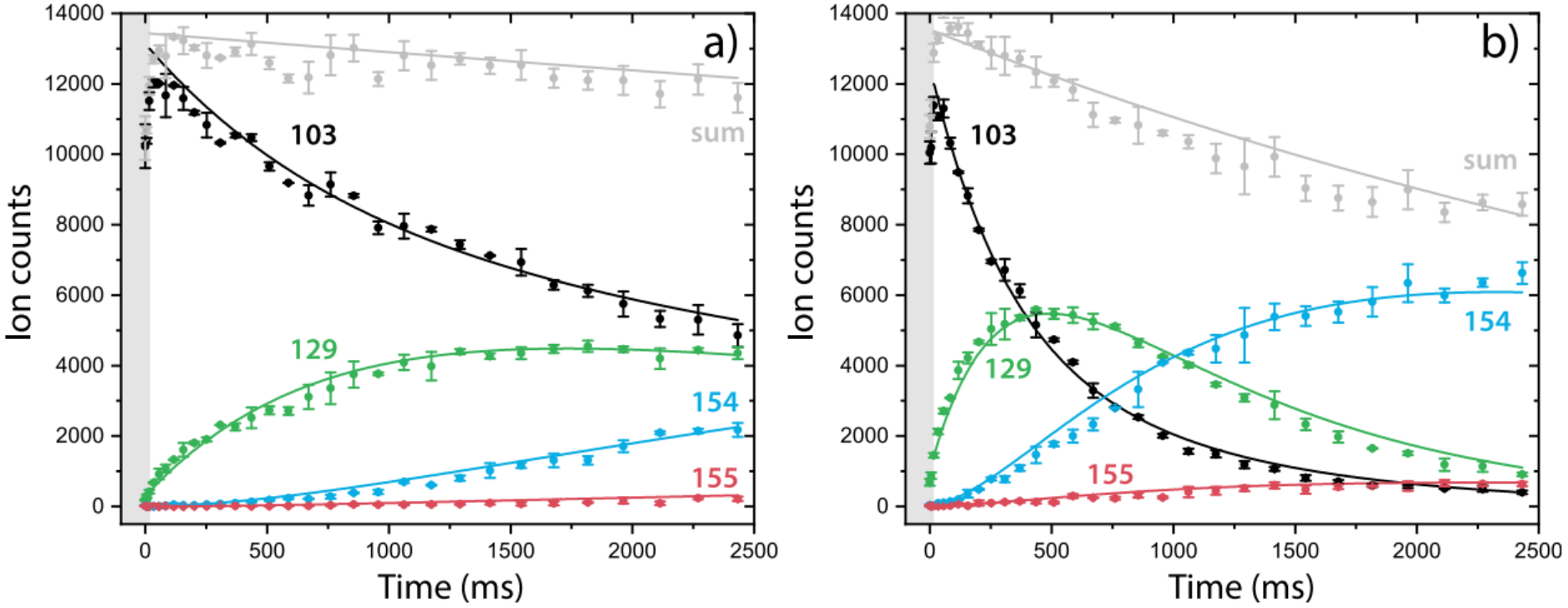

Figure 2. Exemplary kinetic plots of the ion–molecule reaction between benzonitrile$^{\bullet+}$ ($C_6H_5CN^{\bullet+}$) and acetylene (C_2H_2) performed at 150 K for a) low ($1.23(\pm0.14) \times 10^{10}$ cm^{-3}) and b) high ($4.3(\pm0.5) \times 10^{10}$ cm^{-3}) acetylene number density. The experimental ion counts of the reactant benzonitrile$^{\bullet+}$ (black), intermediate m/z 129 (green) and product structures with m/z 154 (blue) and m/z 155 (red) at different trapping times are plotted with dots and error bars. The plots are fitted with an ODE master equation containing the different reaction steps and plotted with a line. The gray dots indicate the sum of all ions and the decay has been implemented into the ODE model to account for the overall ion loss from the trap. The gray box indicates three-body collision conditions due to the He pulse used for trapping the ions in the beginning, these data points were not used in the fitting process.

$$\frac{d[C_7H_5N^{\bullet+}]}{dt} = -k_{RA}[C_7H_5N^{\bullet+}][C_2H_2] + k_{CID}[C_9H_7N^{\bullet+}][C_2H_2 + He]$$

$$\frac{d[C_9H_7N^{\bullet+}]}{dt} = +k_{RA}[C_7H_5N^{\bullet+}][C_2H_2] - k_{RA,C11}[C_9H_7N^{\bullet+}][C_2H_2] - k_{bi}[C_9H_7N^{\bullet+}][C_2H_2] - k_{CID}[C_9H_7N^{\bullet+}][C_2H_2 + He]$$

$$\frac{d[C_{11}H_8N^{+}]}{dt} = +k_{bi}[C_9H_7N^{\bullet+}][C_2H_2]$$

$$\frac{d[C_{11}H_9N^{\bullet+}]}{dt} = +k_{RA,C11}[C_9H_7N^{\bullet+}][C_2H_2]$$

reaction	rate coefficient (cm^3s^{-1})	type	label	number density range C_2H_2 (cm^{-3})
$103^{\cdot+} \rightarrow 129^{\cdot+}$	$3.8(\pm0.4) \times 10^{-11}$	radiative association	k_{RA}	$6.1 \times 10^9 - 2.6 \times 10^{11}$
$129^{\cdot+} \rightarrow 154^{+}$	$1.3(\pm0.3) \times 10^{-11}$	bimolecular	k_{bi}	$6.1 \times 10^9 - 2.6 \times 10^{11}$
$129^{\cdot+} \rightarrow 155^{\cdot+}$	$3.6(\pm0.7) \times 10^{-12}$	radiative association	$k_{RA,C11}$	$1.2 \times 10^{10} - 8.7 \times 10^{10}$

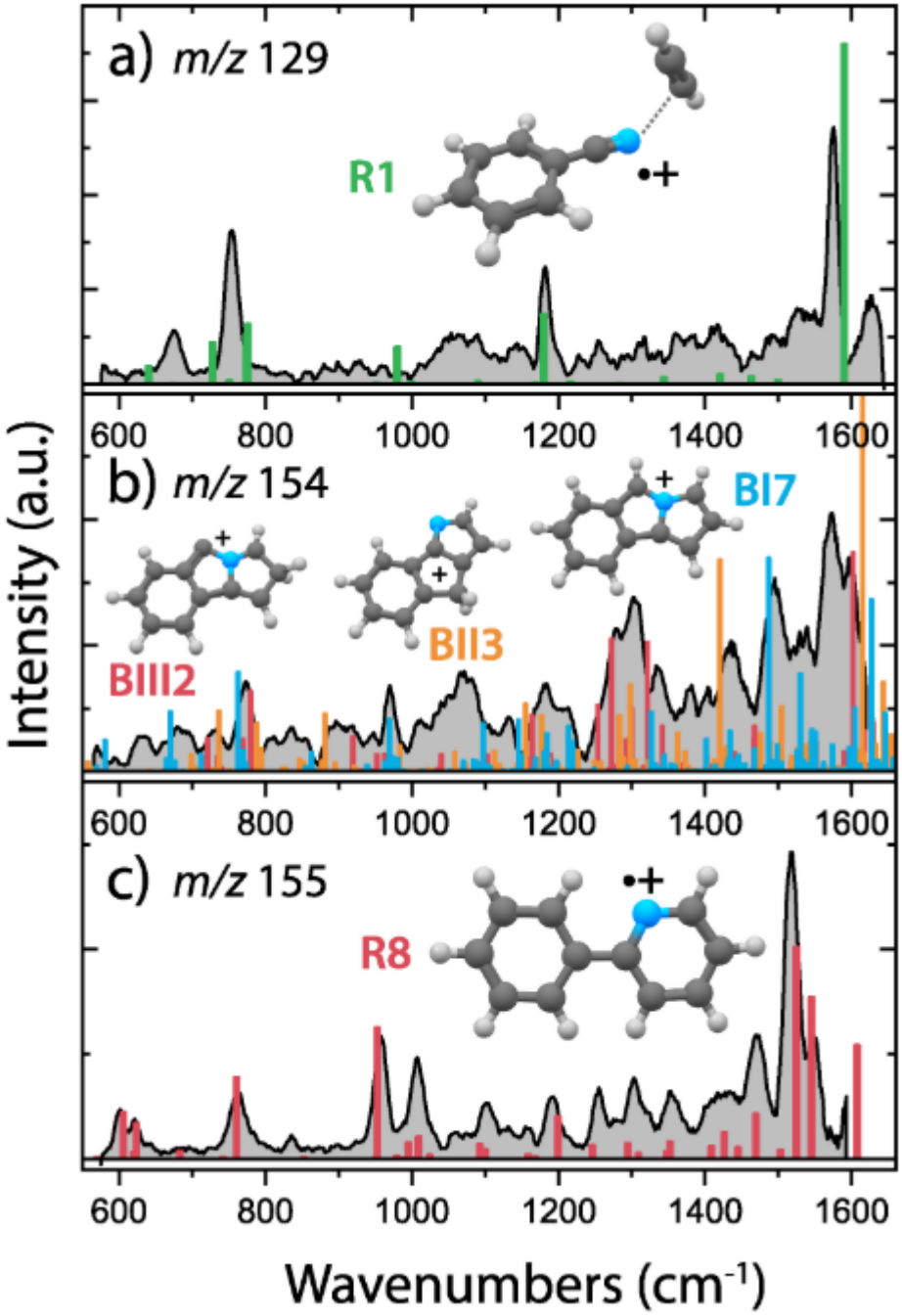

Figure 3. Experimental infrared spectra (gray) of the (a) m/z 129, (b) m/z 154, and (c) m/z 155 reaction intermediates and products of the ion−molecule reaction between benzonitrile$^{\bullet+}$ ($C_6H_5CN^{\bullet+}$) and acetylene (C_2H_2). Calculated infrared frequencies of the assigned structures are shown as sticks for (a) the noncovalent acetylene-benzonitrile$^{\bullet+}$ complex (**R1**, green), (b) benzo-N-pentalene^{+} (**BI7**, blue) and benzo-N-pentaleneCH_2^{+} isomers (**BII3**, orange/**BIII2**, red) and (c) 2-phenylpyridine$^{\bullet+}$ (**R8**, red). The theoretical spectra of the m/z 129 and m/z 155 ions are calculated at the harmonic B3LYP-GD3/6-311++G(2d,p) level of theory, whereas the spectra of the m/z 154 isomers have been calculated at the anharmonic B3LYP-GD3/N07D level of theory.

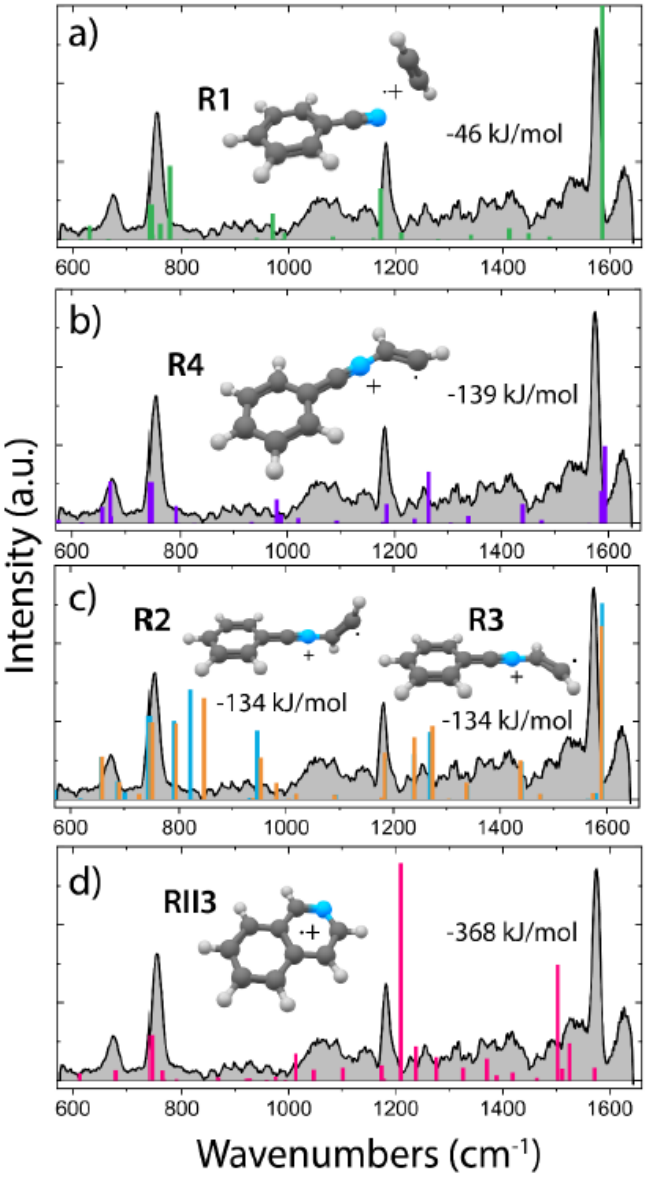

Supplementary Figure 6: Experimental infrared fingerprint spectrum (grey) of the intermediate with *m/z* 129. Calculated vibrational modes are shown for (a) the assigned noncovalent acetylene benzonitrile$^{\bullet+}$ complex (**R1**, green), (b) N-acetylene-benzonitrile$^{\bullet+}$ (**R4**, purple), (c) two N-acetylene-benzonitrile$^{\bullet+}$ conformers (**R2**, **R3**, orange and blue, respectively) and (d) isoquinoline$^{\bullet+}$ (**RII3**, pink). The calculations have been performed at the harmonic B3LYP-GD3/N07D level of theory. The zero-point vibrational energy corrected electronic energies of the molecules are shown relative to the energy of the entrance channel.

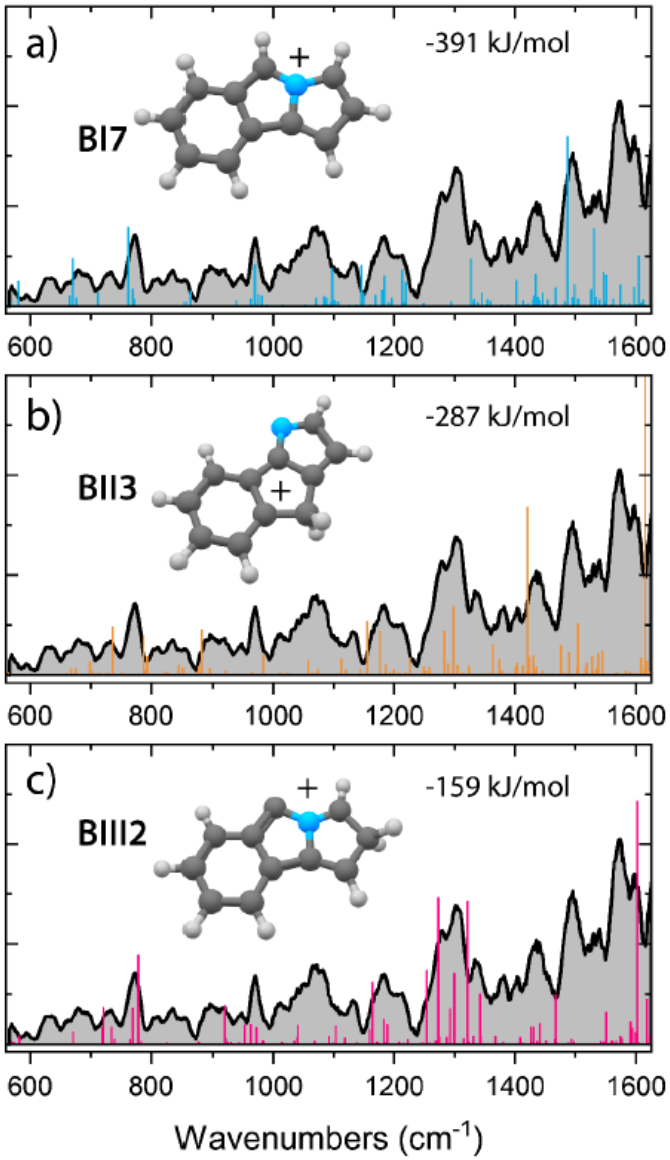

Supplementary Figure 8: Experimental infrared fingerprint spectrum (grey) of the reaction product with *m/z* 154. Calculated anharmonic vibrational modes are shown for (a) benzo-N-pentalene$^+$ (**BI7**, blue), (b) benzo-N-pentaleneCH_2^+ (**BII3**, orange) and (c) a different benzo-N-pentaleneCH_2^+ isomer (**BIII2**, pink). The calculations have been performed at the anharmonic B3LYP-GD3/N07D level of theory. The zero-point vibrational energy corrected electronic energies of the molecules are shown relative to the energy of the entrance channel.

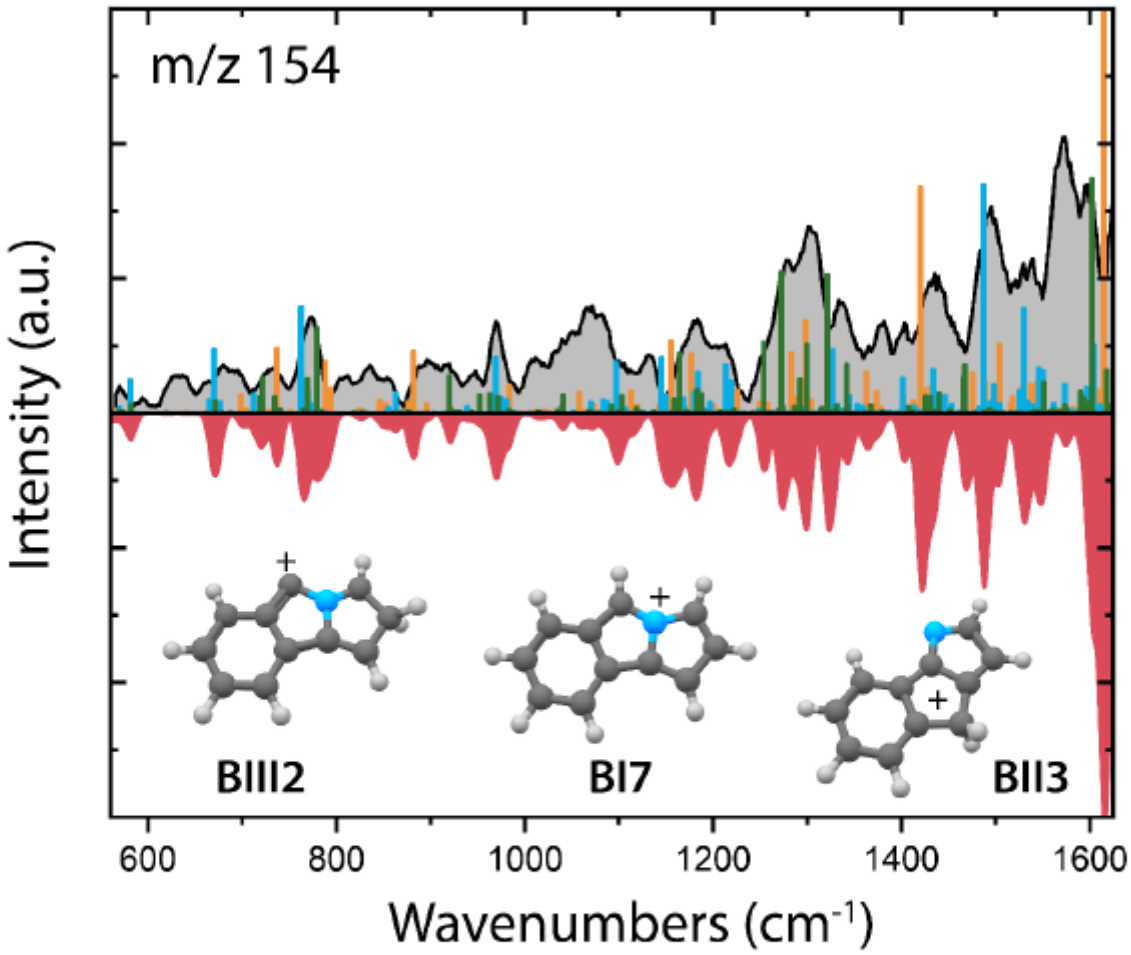

Supplementary Figure 9: Experimental infrared fingerprint spectrum (grey) of the reaction product with *m/z* 154. Calculated anharmonic vibrational modes are shown for the benzo-N-pentalene$^+$ (**BI7**, blue), benzo-N-pentaleneCH_2^+ (**BII3**, orange) and benzo-N-pentaleneCH_2^+ isomer (**BIII2**, green). The calculations have been performed at the anharmonic B3LYP-GD3/N07D level of theory. A convoluted spectrum with equal contributions of all three isomers is shown in red.

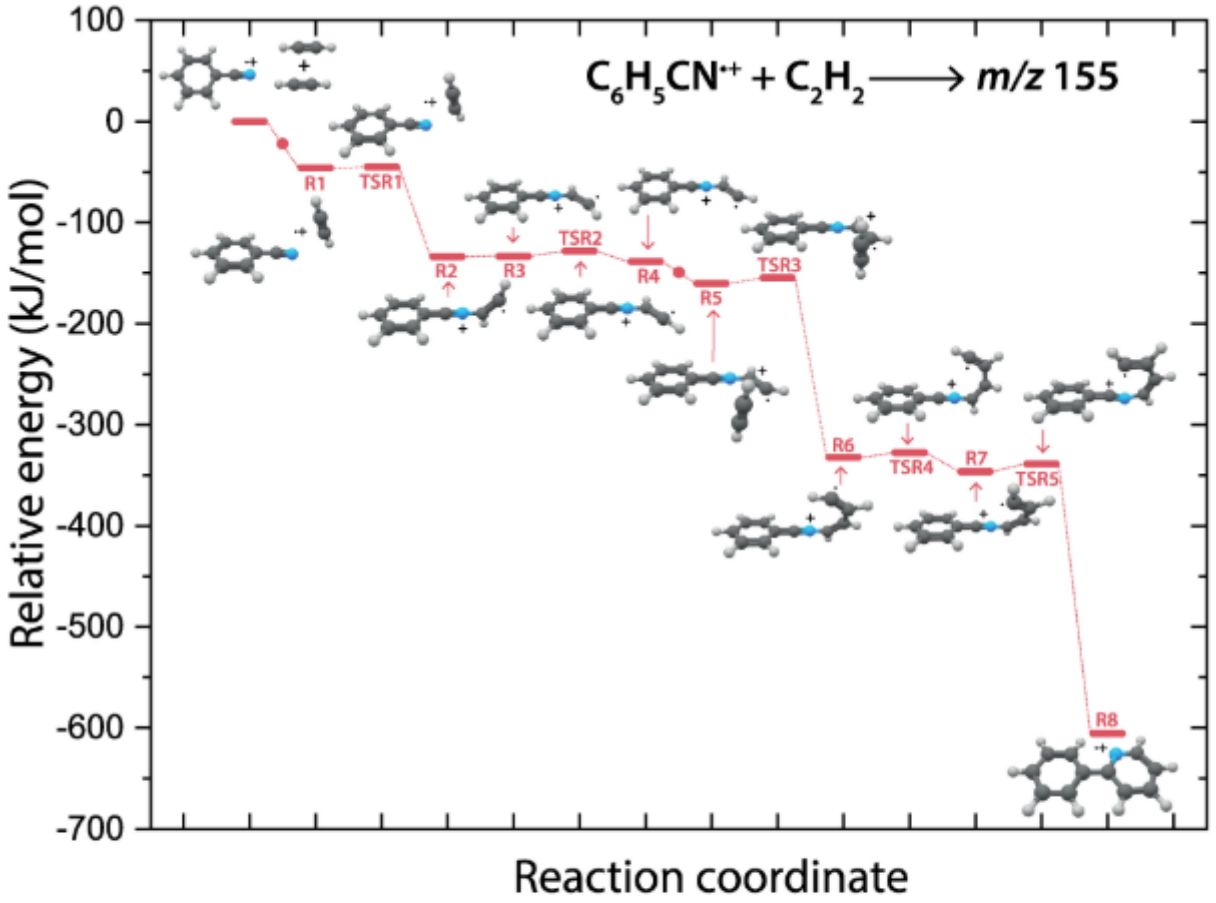

Figure 4. PES of the benzonitrile$^{\bullet+}$ ($C_6H_5CN^{\bullet+}$) with acetylene (C_2H_2) reaction toward the observed 2-phenylpyridine$^{\bullet+}$ (**R8**, m/z 155, red pathway). The small red dots along the pathway display the addition of a new acetylene molecule. The energies are calculated at the B3LYP-GD3/N07D level of theory and are corrected for the zero-point vibrational energy (values are provided in Supporting Table 2).

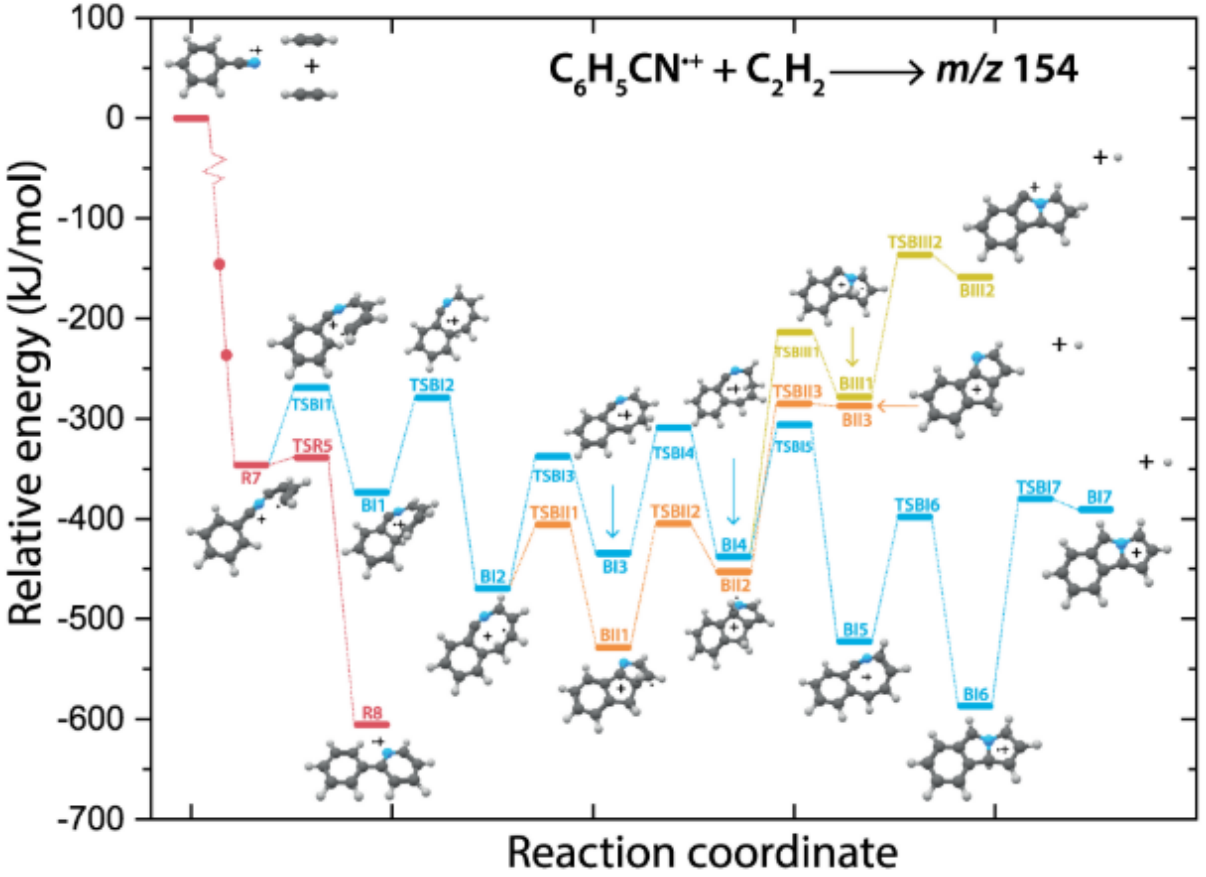

Figure 5. PES of the benzonitrile$^{\bullet+}$ ($C_6H_5CN^{\bullet+}$) with acetylene (C_2H_2) reaction toward the m/z 154 isomers benzo-N-pentalene$^+$ (**BI7**, blue pathway), benzo-N-pentaleneCH_2^+ (**BII3**, orange pathway) and benzo-N-pentaleneCH_2^+ isomer (**BIII2**, yellow pathway). The first part of the reaction pathway (red) up to **R7** follows the calculated path from Figure 4. The small dots along the pathway display the addition of a new acetylene molecule. The energies are calculated at the B3LYP-GD3/N07D level of theory and are corrected for the zero-point vibrational energy (values are provided in Supporting Table 3).

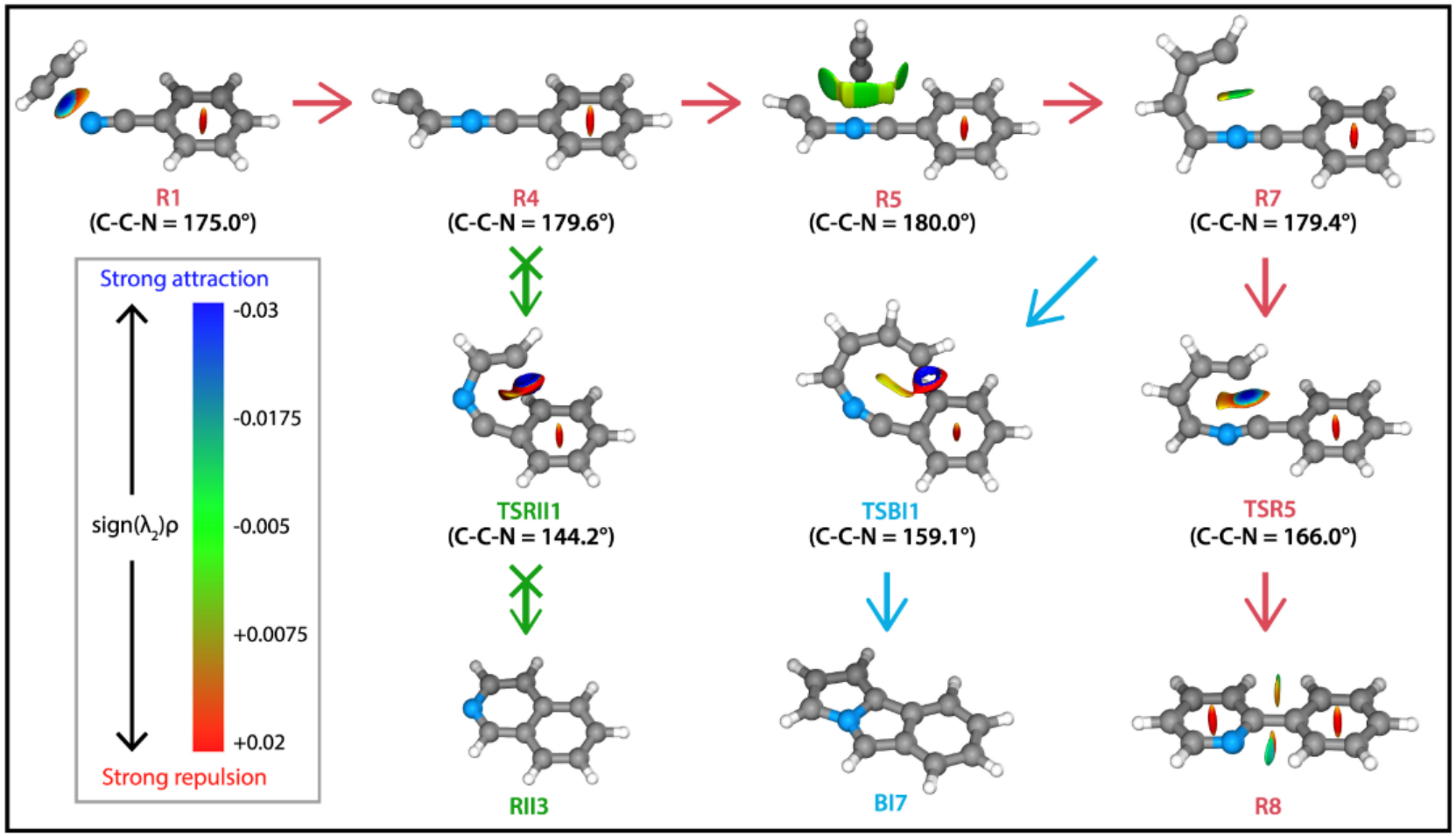

Figure 6. NCI plots of intermediate and transition states of the reaction pathways toward 2-phenylpyridine$^{\bullet+}$ (**R8**, red arrows), benzo-N-pentalene^{+} (**BI7**, blue arrows) and isoquinoline$^{\bullet+}$ (**RII3**, green arrows). The strengths of the NCIs are shown by the color spectrum ranging from red (strong repulsion), green (weak attraction) and blue (strong attraction). The calculated angle of the C−C−N group is shown next to the structures.

Conclusion

- The reactivity of aromatic species is significantly enhanced by the presence of nitrogen heteroatoms as observed here for benzonitrile•+ where the product structures have formed a new N–C bond
- both the first reaction step via the noncovalent prereactive complex (R1) and the sequential reaction toward 2-phenylpyridine•+ proceed via fast radiative association reactions.
- The formation of the cis-isomeric form of the C4H4-group within R7 is favored by attractive vdW forces and thereby favors sequential ring-closure to 2-phenylpyridine•+